Bioorganic Chemistry 90 (2019) 103060

Contents lists available at ScienceDirect

Bioorganic Chemistry

journal homepage: www.elsevier.com/locate/bioorg

New potent antifungal triazole alcohols containing *N*-benzylpiperazine carbodithioate moiety: Synthesis, *in vitro* evaluation and *in silico* study

Yaser Mahmoudi[a], Hamid Badali[b], Seyedeh Mahdieh Hashemi[c], Mahsa Ansari[d], Hamed Fakhim[e], Marjan Fallah[f], Mohammad Shokrzadeh[f], Saeed Emami[c,*]

[a] Student Research Committee, Faculty of Pharmacy, Mazandaran University of Medical Sciences, Sari, Iran
[b] Department of Medical Mycology/Invasive Fungi Research Center, School of Medicine, Mazandaran University of Medical Sciences, Sari, Iran
[c] Department of Medicinal Chemistry and Pharmaceutical Sciences Research Center, Faculty of Pharmacy, Mazandaran University of Medical Sciences, Sari, Iran
[d] Pharmaceutical Sciences Research Center, Student Research Committee, Faculty of Pharmacy, Mazandaran University of Medical Sciences, Sari, Iran
[e] Department of Medical Parasitology & Mycology/Cellular and Molecular Research Center, Urmia University of Medical Sciences, Urmia, Iran
[f] Department of Toxicology and Pharmacology, Faculty of Pharmacy, Mazandaran University of Medical Sciences, Sari, Iran

ARTICLE INFO

Keywords:
Azole antifungals
Antifungal activity
1*H*-1,2,4-triazole
Lanosterol 14α-demethylase

ABSTRACT

A number of 1*H*-1,2,4-triazole alcohols containing *N*-(halobenzyl)piperazine carbodithioate moiety have been designed and synthesized as potent antifungal agents. In vitro bioassays against different *Candida* species including *C. albicans*, *C. glabrata*, *C. parapsilosis*, *C. krusei*, and *C. tropicalis* revealed that the *N*-(4-chlorobenzyl) derivative (**6b**) with MIC values of 0.063–0.5 μg/mL had the best profile of activity, being 4–32 times more potent than fluconazole. Docking simulation studies confirmed the better fitting of compound **6b** in the active site of lanosterol 14α-demethylase (CYP51) enzyme, the main target of azole antifungals. Particularly, the potential of compound **6b** against fluconazole-resistant isolates along with its minimal toxicity against human erythrocytes and HepG2 cells make this prototype compound as a good lead for discovery of potent and safe antifungal agents.

1. Introduction

In recent years, epidemiological studies confirm that the infectious diseases can be caused by bacteria, viruses, fungi or parasites, affecting millions of people worldwide and they are one of the most common causes of morbidity and mortality [1]. These diseases generally can happen to anyone and seem to be conveniently curable, but in particular in most susceptible people with weakened immune system and those hospitalized with tumors, HIV/AIDS and with other serious diseases are often fatal [2]. Excessive use of antimicrobial and immunosuppressive agents leads to an increasing incidence of the multidrug resistant infections and mortality rates [3]. Hence, discovery of new more effective antimicrobials, including antifungal agents is required [4]. Commonly used antifungal drugs are polyenes, azoles, allylamines and echinocandins [5]. Among them, triazoles (such as fluconazole, itraconazole, voriconazole, and posaconazole) are the most interesting class of antifungal drugs because of their broad spectrum, high potency, and having a specific target enzyme [6].

Triazoles act by inhibiting the cytochrome P450 14α-demethylase (CYP51) enzyme. 14α-demethylase is involved in the oxidative demethylation of lanosterol, as a key reaction in the biosynthesis of ergosterol in the fungal cell membrane. The inhibition of ergosterol synthesis leads to the prevention of fungal cell growth or fungal cell death [7].

Studies on the pharmacological properties of triazole antifungals reveal that they have more advantages over imidazoles. The presence of 1,2,4-triazole ring (instead of imidazole) with increased polarity resulted in improving solubility and decreasing the binding to plasma proteins, as well as better specificity of these drugs for fungal enzymatic systems [6,8].

Among the triazole antifungals, fluconazole is the most widely used worldwide because of its low toxicity, excellent safety profile, and linear pharmacokinetics. However, some drawbacks of this drug have encouraged medicinal chemists for design and discovery of novel antifungal agents based on the triazole alcohol structure of fluconazole [9]. Structurally, the difference between newer azole antifungals and fluconazole mainly lies on the type of side chain attached to the carbinol center of triazole alcohol scaffold. Accordingly, most of the recent efforts aim to optimize this part of molecule, which can be well accommodated in the hydrophobic pocket of target enzyme, 14α-

* Corresponding author.
E-mail addresses: semami@mazums.ac.ir, sdemami12@gmail.com (S. Emami).

https://doi.org/10.1016/j.bioorg.2019.103060
Received 16 November 2018; Received in revised form 26 May 2019; Accepted 7 June 2019
Available online 12 June 2019

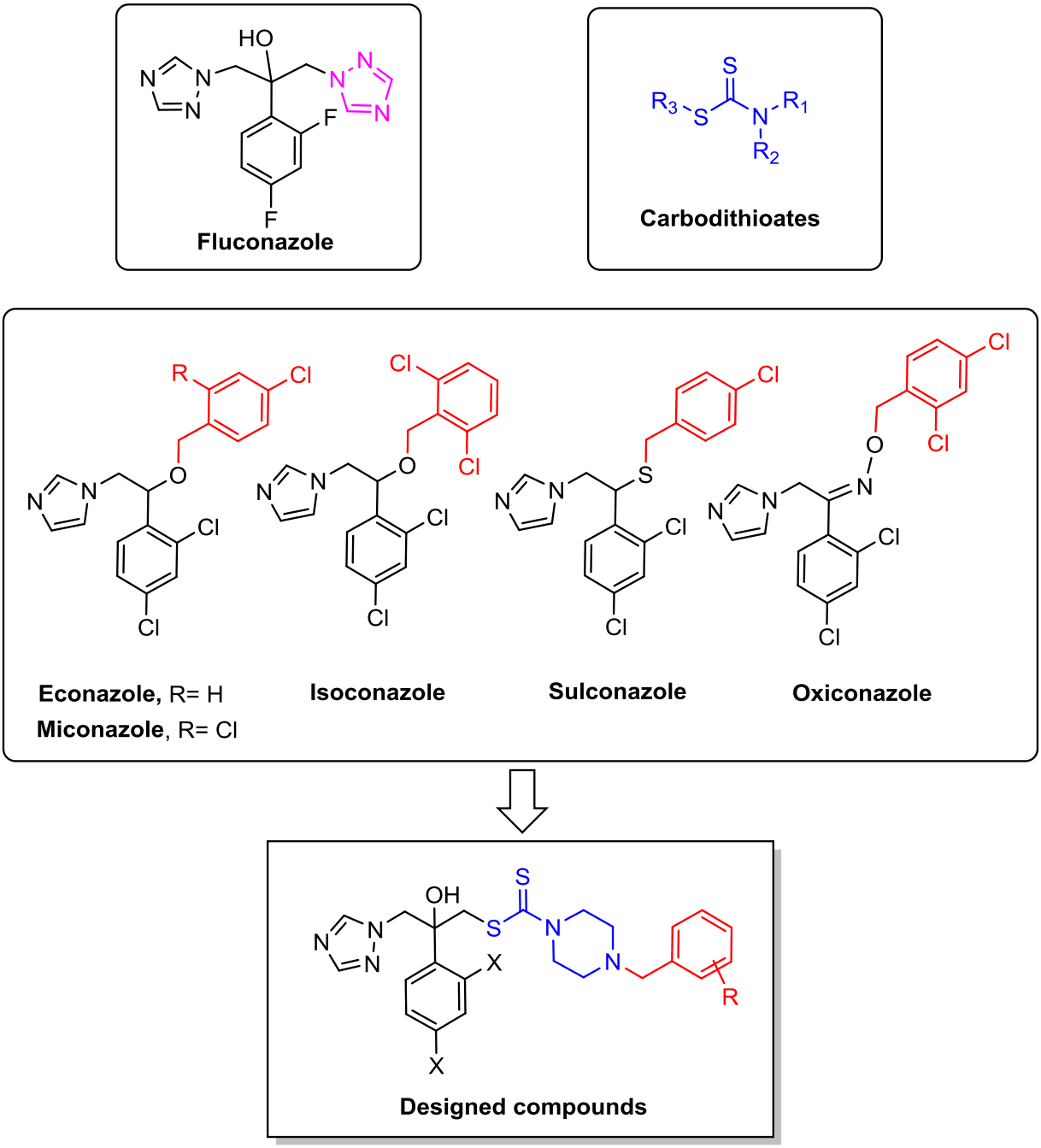

Fig. 1. Design of new antifungal triazole alcohols derived from fluconazole containing *N*-benzylpiperazine carbodithioate moiety.

demethylase [10].

On the other hand, carbodithioate (or dithiocarbamate) has been considered as a versatile functional group in the bioactive compounds. In particular, carbodithioates have been used as fungicide in agriculture extensively [11]. Recently, a series of azole-carbodithioate hybrids have been synthesized and evaluated by Kumar and co-workers as vaginal anti-*Candida* contraceptive agents [12]. Monti et al. investigated a number of *N*-mono- and *N*,*N*-disubstituted carbodithioates against three β-carbonic anhydrases from the fungal pathogens, *Candida albicans*, *Candida glabrata*, and *Cryptococcus neoformans*. Their results showed that carbodithioates can strongly inhibit the beta-class fungal carbonic anhydrases at subnanomolar to the micromolar range [13].

In continuation of our work on fluconazole modified antifungal agents [14–16], we designed a new series of triazole alcohols containing *N*-benzylpiperazine carbodithioate moiety (Fig. 1). Indeed, one triazole ring of fluconazole has been substituted by *N*-(halobenzyl)piperazine carbodithioate scaffold. The (substituted)benzyl part of the designed molecules is found in several azole antifungals including miconazole, econazole, oxiconazole, isoconazole and sulconazole (Fig. 1). It has been postulated that the *N*-(halobenzyl)piperazine carbodithioate side chain attached to the carbinol center of triazole alcohol can be well accommodated in the hydrophobic pocket of target enzyme 14α-demethylase. Thus we report here synthesis, antifungal activity and molecular docking of new triazole alcohols **6a–i** containing *N*-(halobenzyl) piperazine carbodithioate moiety.

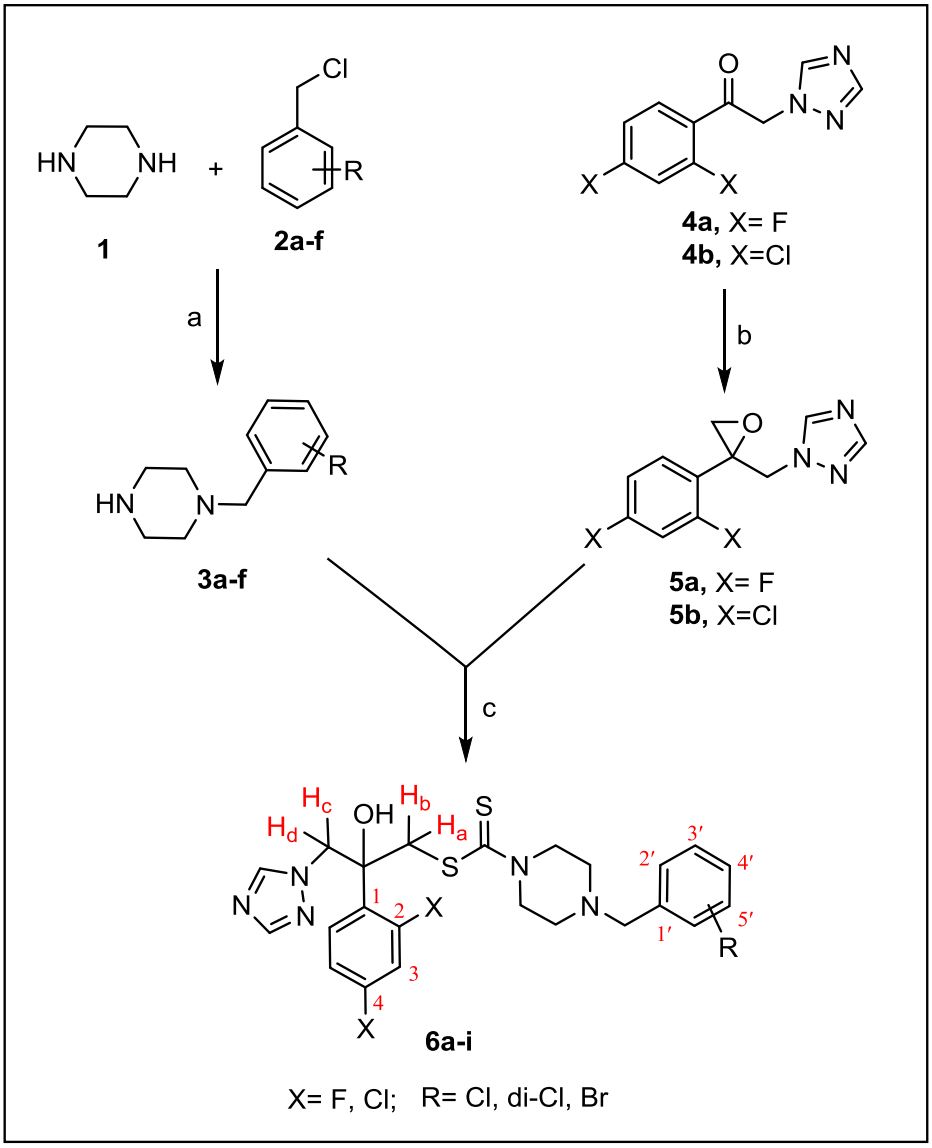

Scheme 1. Synthesis of the title compounds **6a–i**. Reagents and conditions: (a) EtOH, reflux, 2 h, (b) TMSI, NaOH, toluene, 60 °C, 3 h; (c) TEA, CS_2, EtOH.

2. Results and discussion

2.1. Chemistry

The target compounds **6a–i** were synthesized following the synthetic route illustrated in Scheme 1. The intermediate *N*-benzylpiperazine derivatives **3a–f** were obtained by the reaction of benzyl chloride derivatives **2a–f** with the excess of piperazine in refluxing ethanol. On the other hand, the oxirane derivatives **5a,b** were prepared from the desired phenacyltriazole (**4a** or **4b**) in the presence of trimethylsulfoxonium iodide and NaOH 20% in toluene. The final compounds **6a–i** were synthesized by the sequential one-pot reaction of *N*-benzylpiperazine derivatives **3a–f**, carbon disulfide and oxiranes (**5a** or **5b**) in the presence of triethylamine (TEA) in ethanol. Accordingly, the *in situ* generated carbodithioate salt underwent ring opening reaction with oxirane to afford desired carbodithioate alcohol **6**. The structural assignments of new compounds were based on their spectral data (IR, NMR, and MS) as reported in the Experimental section.

2.2. Antifungal activity against fluconazole-susceptible and fluconazole-susceptible dose-dependent Candida species

Clinically, *Candida albicans* is one of the major pathogens in immunocompromised patients. Recent epidemiological investigations demonstrated that fungal infections shift towards non-albicans *Candida* species with increasing resistant to the available antifungal agents. The most prominent non-albicans species are *C. glabrata*, *C. parapsilosis*, *C. krusei*, and *C. tropicalis*, which being responsible for more incidence of invasive candidiasis respect to *C. albicans* [17,18]. Accordingly, the *in vitro* antifungal susceptibility testing of final compounds **6a–i** were performed against *C. albicans* and non-albicans species including *C. glabrata*, *C. parapsilosis*, *C. krusei*, and *C. tropicalis* by using broth microdilution method [19,20]. The obtained MIC (minimum inhibitory concentration) values of tested compounds in comparison with fluconazole as standard antifungal drug are summarized in Table 1.

As observed in Table 1, all of tested compounds exhibited significant inhibitory activity against fluconazole-susceptible and fluconazole-susceptible dose-dependent *Candida* species (MICs ≤ 4 μg/mL). A survey on obtained results revealed that *N*-(4-chlorobenzyl) derivative **6b** with MIC values of 0.063–0.5 μg/mL was the most potent compound. The antifungal potency of this derivative was 4–32 times greater

Table 1
The MIC values (μg/mL) of compounds **6a–i** against fluconazole-susceptible and fluconazole-susceptible dose-dependent isolates of *Candida* species.[a]

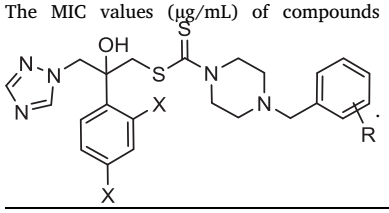

Compound	X	R	*C. a.*	*C. g.* (I)	*C. g.* (II)	*C. g.* (III)	*C. g.* (IV)	*C. p.* (I)	*C. p.* (II)	*C. p.* (III)	*C. k.*	*C. t.*
6a	F	3-Cl	0.125	0.25	1	0.5	0.5	0.063	0.063	0.25	0.25	0.5
6b	F	4-Cl	0.5	0.063	0.5	0.5	0.5	0.063	0.063	0.063	0.125	0.5
6c	F	2,4-Cl_2	0.125	0.5	8	4	4	0.5	0.5	2	4	0.5
6d	F	3,4-Cl_2	0.5	2	1	0.5	0.5	0.125	0.125	0.25	0.25	1
6e	F	2,6-Cl_2	0.25	0.25	2	1	1	0.125	0.25	0.25	1	1
6f	F	4-Br	0.25	0.063	4	2	1	0.125	0.063	0.25	0.5	1
6g	Cl	3-Cl	0.25	0.5	4	2	2	1	0.25	0.5	0.25	16
6h	Cl	2,4-Cl_2	0.25	1	4	2	4	1	1	0.5	2	32
6i	Cl	3,4-Cl_2	0.5	1	2	2	1	1	1	0.5	0.5	32
Fluconazole			1	2	4	4	2	0.5	0.5	1	4	4

[a] *C. a.*: *C. albicans* (IFRC 194); *C. g.* (I): *C. glabrata* (IFRC 339); *C. g.* (II): *C. glabrata* (IFRC 1274); *C. g.* (III): *C. glabrata* (IFRC 1275); *C. g.* (IV): *C. glabrata* (IFRC 1276); *C. p.* (I): *C. parapsilosis* (IFRC 1269); *C. p.* (II): *C. parapsilosis* (IFRC 1270); *C. p.* (III): *C. parapsilosis* (IFRC 1271); *C. k.*: *C. krusei* (IFRC 1012); *C. t.*: *C. tropicalis* (IFRC 1057).

than that of the standard drug fluconazole. Furthermore, the 3-chlorobenzyl analog **6a** had a good profile of activity against both albicans and non-albicans species of *Candida*.

The most of compounds listed in Table 1, contain 2,4-difluorophenyl as found in the fluconazole structure. However, a limited series of 2,4-dichlorophenyl analogs were also synthesized and tested. The latter pharmacophoric part could be found in imidazole antifungals i.e., miconazole and in triazole drugs such as terconazole and itraconazole. In general, the obtained MICs in our study indicated that 2,4-difluorophenyl derivatives were more potent than their dichlorophenyl analogs.

As mentioned in introduction, some imidazole antifungals possess mono- or di-halosubstituted benzyl moiety as side chain. Thus in our SAR study, the attached benzyl moiety to the piperazine ring was altered by mono- and dihalo-substitution. In general, the mono-chlorobenzyl derivatives (**6a** and **6b**) were inherently potent antifungal compounds. However, replacement of chlorine with bromine in compound **6b** resulted in compound **6f** with same or lower activity. Thus, 4-chloro is more preferred than 4-bromo substituent. Introduction of second chlorine atom on benzyl group also had no positive effect as observed with dichlorobenzyl derivatives **6c–e**, **6 h** and **6i**.

2.3. Antifungal activity against fluconazole-resistant Candida species

As resistance to the currently available antifungal agents such as fluconazole is emerging in many of *Candida* species, thus the antifungal effect of all synthesized compounds was also investigated against fluconazole-resistant species of *Candida* including *C. albicans* ($n = 3$), *C. parapsilosis* ($n = 1$) and *C. krusei* ($n = 2$). The results were presented as MIC values in Table 2. The MIC values of fluconazole against *C. albicans* and *C. krusei* isolates were ≥64 μg/mL. The representative compound **6b** effectively inhibited the growth of *C. albicans* and *C. krusei* isolates at the concentrations of 2–16 μg/mL. The MIC of this compound against *C. parapsilosis* was 2 μg/mL, being significantly lower than that of fluconazole (MIC ≥ 8 μg/mL). The most potent compounds were **6d** and **6f** (MIC = 0.25 μg/mL), displaying 32-time higher potency compared to fluconazole against *C. parapsilosis*. Moreover, the remaining compounds were also significantly more potent than fluconazole against *C. parapsilosis*. Overall, compound **6b** showed good profile of activity against fluconazole-resistant species of *Candida*.

Table 2
The MIC values (μg/mL) of compounds **6a-i** against fluconazole-resistant isolates.

Compound	*C. a.* IFRC 1260	*C. a.* IFRC 1261	*C. a.* IFRC 1262	*C. p.* IFRC 84	*C. k.* IFRC 1280	*C. k.* IFRC 1281
6a	32	32	16	0.5	32	32
6b	16	16	8	2	2	16
6c	32	32	32	2	32	32
6d	32	32	32	0.25	32	32
6e	32	32	32	1	64	32
6f	16	32	16	0.25	32	32
6g	64	64	64	0.5	64	64
6h	64	64	64	1	64	64
6i	64	64	64	1	64	64
Fluconazole	≥64	≥64	≥64	≥8	≥64	≥64

Abbreviations: *Candida albicans* (IFRC 1260); *Candida albicans* (IFRC 1261); *Candida albicans* (IFRC 1262); *Candida parapsilosis* (IFRC 84); *Candida krusei* (IFRC 1280); *Candida krusei* (IFRC 1281).

2.4. Toxicity of compound **6b** against erythrocytes

In order to check the safety profile of designed compounds, the toxicity of representative compound **6b** was evaluated against human erythrocytes by determining their hemolytic activity. The compound was tested at different concentrations of 1, 10 and 50 μg/mL, in comparison with standard antifungal agent fluconazole and positive control Triton X-100. As observed in Fig. 2, while triton X-100 produced 100% hemolysis, only a limited hemolysis occurred following exposure to compounds **6b** at the higher concentration of 50 μg/mL. Compound **6b** as well as fluconazole showed no significant hemolytic activity at the concentrations of 1 and 10 μg/mL compared to negative control. Therefore, the promising compound **6b** displayed minimal toxicity against human erythrocytes at the antifungal MIC values.

2.5. Effect of compounds **6b** on the viability of HepG2 cells

An important issue in the discovery of new antifungal agents is selectivity against fungi cells and proper safety profile towards host cells. As reported previously, azole antifungals might have liver toxicity [21,22]. Thus we next investigated the effect of selected compound **6b** on the viability of human hepatoma cells HepG2. The MTT assay result of compound **6b** on HepG2 cells was depicted in Fig. 3. As seen in

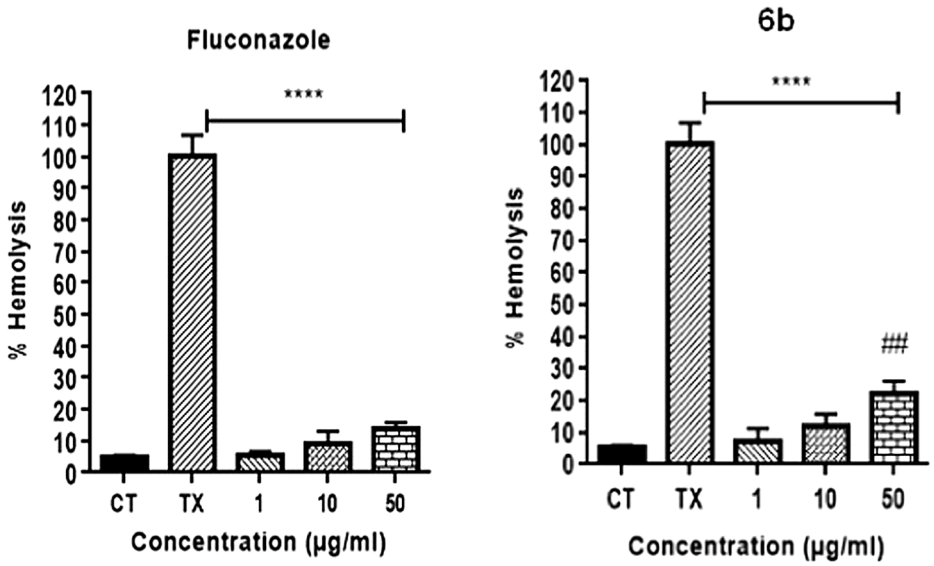

Fig. 2. Hemolytic activity of compound **6b** and fluconazole against human erythrocytes at the concentrations of 1, 10 and 50 µg/mL. The negative control (CT) consisted of erythrocytes treated with DMSO and the positive control consisted of erythrocytes treated with Triton X-100 (TX, 2% v/v).

Fig. 3, the viability of HepG2 cells for this compound was affected less than 50% at the concentrations of 25, 50 and 100 µg/mL. Accordingly, the IC_{50} value of test compound against HepG2 cell line was > 100 µg/mL, being similar to that of fluconazole. As our compound can inhibit the growth of *Candida* species at concentrations ≤0.5 µg/mL, thus it has favorable safety profile.

2.6. Docking study

The key enzyme in the ergosterol biosynthetic pathway namely lanosterol 14α-demethylase (CYP51) is the main target of azole antifungals [6]. The similar structure of our compounds with azole antifungals prompted us to investigate their interactions with CYP51 enzyme in comparison with fluconazole. Accordingly, the binding mode of the promising compound **6b** was studied by docking simulation. The structures of CYP51 enzymes originated from *C. glabrata* and *C. albicans* (CGCYP51 and CACYP51, respectively) were used for computational studies. Before simulation study of the target compound, we validated the precision of our docking protocol. Towards this end, the cognate ligand itraconazole was removed from the binding site and re-docked. We found a good fitting between the localization of the itraconazole upon docking and that of crystal structure as evidenced from the root mean square deviation values of 1.58 and 1.71 Å for CGCYP51 and CACYP51, respectively.

Docking experiments were carried out on both (*R*)- and (*S*)-enantiomers of the selected compound. Both stereoisomers interacted with CYP51 through a similar binding mode. As shown in Fig. 4, (*R*)-**6b** binds to the active site of CGCYP51 with a binding energy of −10.17 kcal/mol and a coordinated bond forming distance 2.51 Å away from the heme iron. In the case of CACYP51, the binding energy was −9.66 kcal/mol and the N_4 atom of triazole nucleus of the compound (*R*)-**6b** was coordinated to the heme iron of CACYP51 with a bond distance of 2.31 Å. It should be noted that the binding energy and coordination bond distance for fluconazole were −6.27 kcal/mol and 2.31 Å, respectively. As depicted in Fig. 5, the difluorophenyl moiety of the molecule (*R*)-**6b** is located in a hydrophobic pocket and interacts with Phe228, Gly303, Ile304, Phe126, Ile131, Thr122 and Tyr132. The piperazinyl part interacts with the surrounding hydrophobic amino acid residues including Leu376, Phe380, Ile379, and Tyr118. The terminal 4-chlorobenzyl group binds through the hydrophobic and van der Waals interactions with His377, Pro375 and Met508. The carbodithioate and triazole moieties were found to be in contact with Leu121 and Thr311, respectively. It would appear that the hydrophobic interaction with a larger hydrophobic side chain residue of compound **6b** is

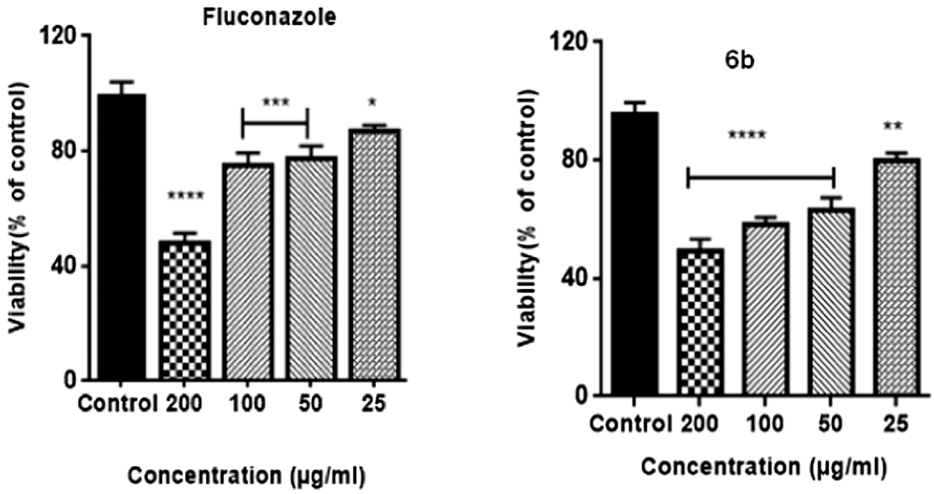

Fig. 3. Cytotoxic activity of compound **6b** and fluconazole against HepG2 cells at the concentrations of 25, 50, 100 and 200 µg/mL.

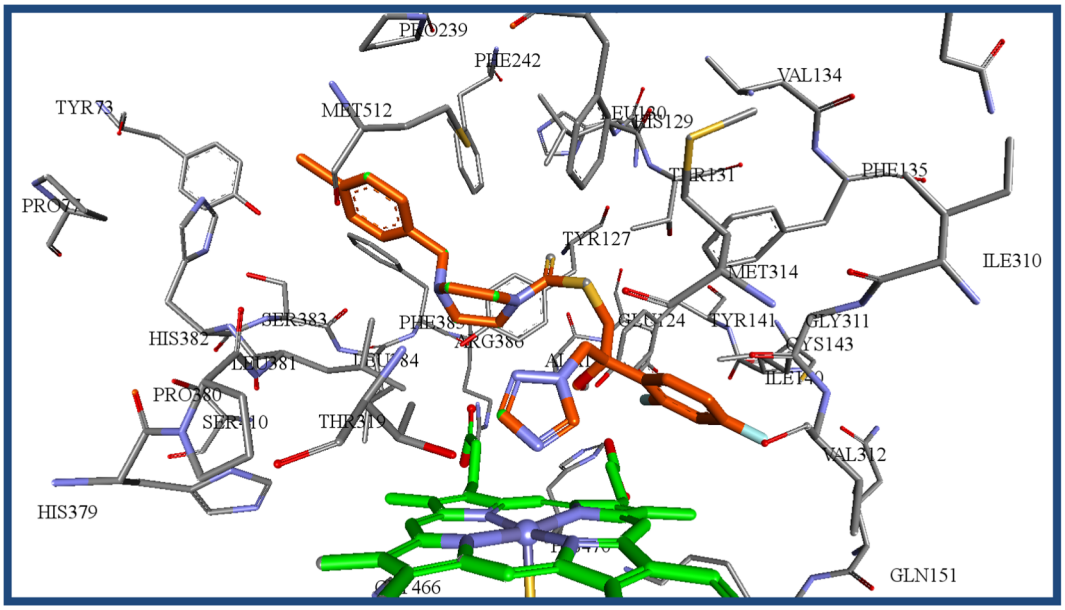

Fig. 4. 3D presentation of docked (*R*)-**6b** in the active site of CGCYP51 lanosterol 14α-demethylase.

responsible for the more potent inhibitory activity of the prototype compound respect to fluconazole.

3. Conclusion

We have designed and synthesized a number of triazole alcohol-based antifungals by incorporating *N*-benzylpiperazine carbodithioate moiety into the phamacophoric framework of fluconazole. In vitro bioassays against fluconazole-susceptible and fluconazole-susceptible dose-dependent *Candida* species revealed that all compounds had potent activity against *C. albicans*, *C. glabrata*, *C. parapsilosis*, *C. krusei*, and *C. tropicalis*, with MIC values ≤ 4 μg/mL. The *N*-(4-chlorobenzyl) derivative (**6b**), displaying MIC values of 0.063–0.5 μg/mL was the best one. Its activity was 4–32 times higher than that of fluconazole. SAR analysis demonstrated that the 2,4-difluorophenyl-carbinol is more favorable than 2,4-dichlorophenyl-carbinol scaffold. Further evaluation against fluconazole-resistant isolates indicated that compound **6b** was active towards *C. albicans*, *C. krusei* and *C. parapsilosis* isolates, displaying MIC values of 2–16 μg/mL. Toxicity assays against human erythrocytes and HepG2 cells demonstrated the favorable therapeutic window of this prototype compound comparable to standard drug fluconazole. Docking simulation studies confirmed the proper accommodation of compound **6b** in the active sites of lanosterol 14α-demethylase (CYP51) enzymes originated from *C. glabrata* and *C. albicans*, being in accordance to the greater activity of compound **6b** respect to fluconazole.

4. Experimental

The intermediate compounds **4a,b** and **5a,b** were synthesized according to the literature methods [14,23].

4.1. General procedure for the preparation of N-benzylpiperazine derivatives *3a–f*

A solution of appropriate benzyl chloride derivative **2a–f** (1.0 mmol) and piperazine (3.0 mmol) in ethanol (10 mL) was refluxed for 2 h. After consumption of the benzyl chloride derivative (checked by TLC, solvent *n*-hexane), and cooling of the reaction mixture, water (10 mL) was added. Then, the mixture was extracted with ethyl acetate 3 times and the organic layers were combined and dried (Na_2SO_4). After evaporation of the solvent under reduced pressure, the desired product **3a–f** was obtained which was use without further purification.

4.2. General procedure for the preparation of compounds *6a–i*

To a mixture of benzylpiperazine derivatives **3a–f** (1 mmol) in ethanol (10 mL), triethylamine (1 mmol) and carbon disulfide (3 mmol) was added and stirred in an ice bath for 2 h. After consumption of starting materials **3a–f**, oxiran derivative (**5a** or **5b**, 1 mmol) was added and the reaction mixture allowed to stir at room temperature for 24 h. After the completion of the reaction, water (10 mL) was added and the mixture was left in refrigerator overnight. The precipitated solid was collected and washed with water and then recrystallized from *n*-hexane-diethyl ether to give pure compounds **6a–i**.

4.2.1. 2-(2,4-Difluorophenyl)-2-hydroxy-3-(1H-1,2,4-triazol-1-yl)propyl 4-(3-chlorobenzyl)piperazine-1-carbodithioate (*6a*)

Yield: 66%; mp: 116–118 °C; IR (ν_{max}, cm^{-1}): 3204, 3068, 2793, 2756, 1616, 1598, 1502, 1423, 1251, 1247, 1220, 1143, 1129, 966, 676, 526. ^{1}H NMR (400 MHz, $CDCl_3$) δ: 2.47–2.58 (m, 4H, piperazine), 3.52 (s, 2H, CH_2 benzylic), 3.85–3.98 (m, 2H, piperazine), 4.01 (d, 1H, J = 15.2 Hz, H_a), 4.29 (d, 1H, J = 15.2 Hz, H_b), 4.31–4.43 (m, 2H, piperazine), 4.68 (d, 1H, J = 14.0 Hz, H_c), 4.72 (d, 1H, J = 14.4 Hz, H_d), 5.33 (s, 1H, OH), 6.8–6.88 (m, 2H, H-3 and H-5), 7.17–7.21 (m, 1H, H-6′), 7.23–7.28 (m, 2H, H-4′ and H-5′), 7.34 (d, 1H, J = 0.8 Hz, H-2′), 7.56–7.61 (m, 1H, H-6), 7.85 (s, 1H, triazole), 8.14 (s, 1H, triazole). ^{13}C NMR (100 MHz, DMSO-d_6) δ: 46.60 (d, $J_{C,F}$ = 3.8 Hz, CH_2-S), 50.17 (1C, piperazine), 52.32 (2C, piperazine), 52.99 (1C, piperazine), 56.81 (C-OH), 60.87 (CH_2 benzylic), 73.75 (CH_2-N), 104.56 (dd, $J_{C,F}$ = 25.6 and 27.2 Hz, 2,4-F_2Ph C-3), 111.33 (d, $J_{C,F}$ = 20.8 Hz, 2,4-F_2Ph C-5), 125.42 (dd, $J_{C,F}$ = 12.7 and 3.4 Hz, 2,4-F_2Ph C-1), 127.57 (C-5′), 127.99 (C-6′), 129.00 (C-4′), 130.54 (d, $J_{C,F}$ = 8.7 Hz, 2,4-F_2Ph C-6), 130.58 (C-2′), 133.45 (C-3′), 140.79 (C-1′), 145.45 (C-5 triazole), 151.11 (C-3 triazole), 159.41 (dd, $J_{C,F}$ = 246.3 and 12.4 Hz, 2,4-F_2Ph C-2), 162.40 (dd, $J_{C,F}$ = 244.9 and 12.4 Hz, 2,4-F_2Ph C-4), 195.09 (C=S). MS (*m/z*, %): 523 (M^+, < 1), 334 (8), 221 (10), 209 (36), 182 (8), 168 (13), 154 (37), 139 (13), 125 (100), 89 (17), 56 (6). Anal. Calcd for $C_{23}H_{24}ClF_2N_5OS_2$: C, 52.72; H, 4.62; N, 13.36. Found: C, 52.55; H, 4.63; N, 13.30.

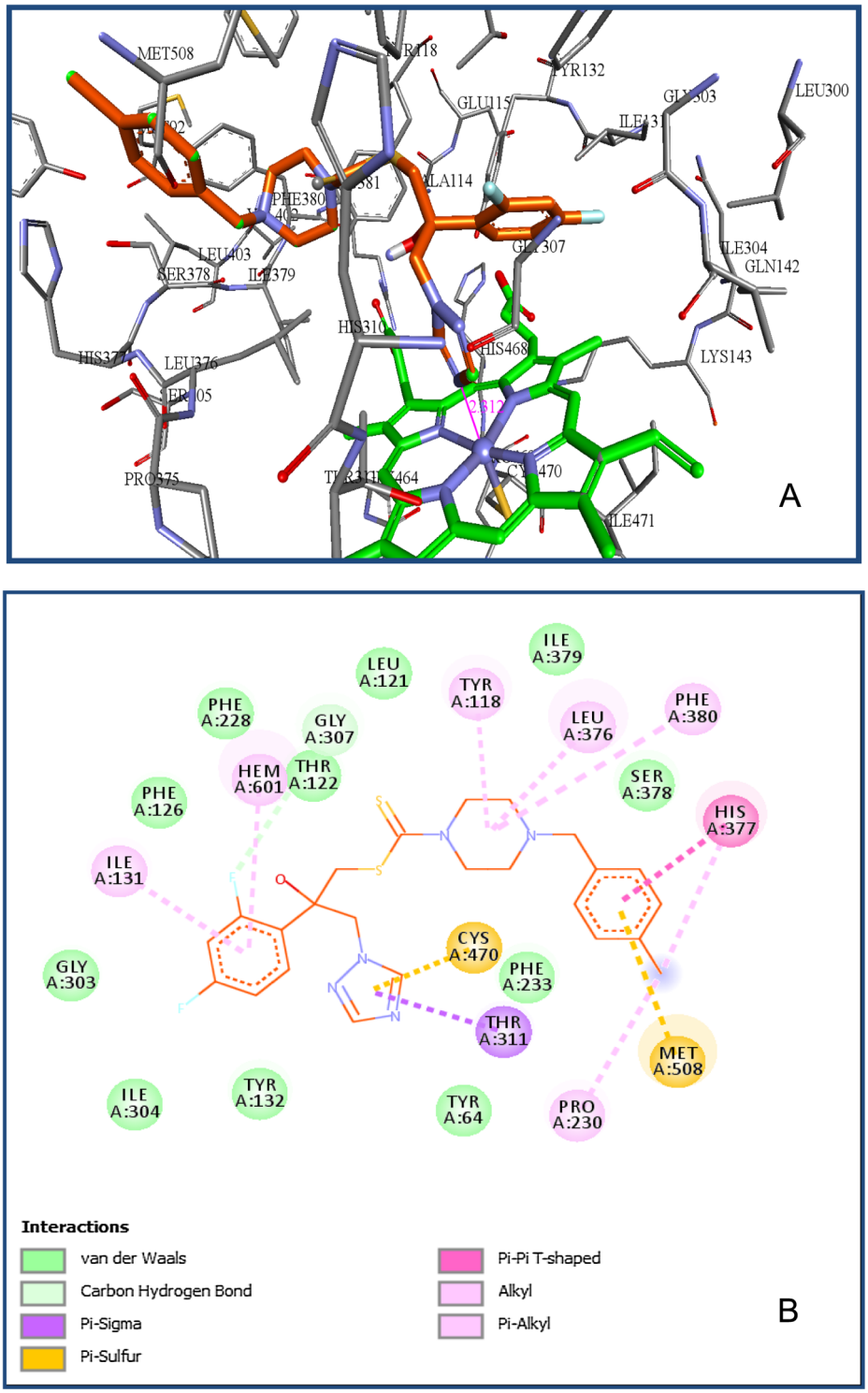

Fig. 5. (A) 3D presentation of docked (*R*)-**6b** in the active site of CACYP51 lanosterol 14α-demethylase; (B) 2D presentation for the binding mode of (*R*)-**6b** with amino acids in the active site of CACYP51 lanosterol 14α-demethylase.

*4.2.2. 2-(2,4-Difluorophenyl)-2-hydroxy-3-(1H-1,2,4-triazol-1-yl)propyl 4-(4-chlorobenzyl)piperazine-1-carbodithioate (**6b**)*

Yield: 64%; mp: 134–136 °C; IR (ν_{max}, cm^{-1}): 3208, 3069, 2914, 1615, 1502, 1461, 1274, 1224, 1114, 1027, 1030, 966, 848, 676, 479. ^{1}H NMR (400 MHz, $CDCl_3$) δ: 2.47–2.55 (m, 4H, piperazine), 3.51 (s, 2H, CH_2 benzylic), 3.85–3.98 (m, 2H, piperazine), 4.01 (d, 1H, J = 14.8 Hz, H_a), 4.29 (d, 1H, J = 15.2 Hz, H_b), 4.31–4.42 (m, 2H, piperazine), 4.67 (d, 1H, J = 14.0 Hz, H_c), 4.72 (d, 1H, J = 14.0 Hz, H_d), 5.32 (s, 1H, OH), 6.80–6.87 (m, 2H, H-3 and H-5), 7.26 (d, 2H, J = 8.8 Hz, H-2′ and H-6′), 7.32 (d, J = 8.4 Hz, 2H, H-3′ and H-5′), 7.55–7.62 (m, 1H, H-6), 7.85 (s, 1H, triazole), 8.13 (s, 1H, triazole). ^{13}C NMR (100 MHz, DMSO-d_6) δ: 46.54 (CH_2-S), 50.20 (1C, piperazine), 52.29 (2C, piperazine), 52.94 (1C, piperazine), 56.80 (C-OH), 61.57 (CH_2 benzylic), 73.73 (CH_2-N), 104.55 (dd, $J_{C,F}$ = 24.9 and 27.4 Hz, 2,4-F_2Ph C-3), 111.36 (d, $J_{C,F}$ = 20.3 Hz, 2,4-F_2Ph C-5), 125.41 (dd, $J_{C,F}$ = 12.2 and 3.5 Hz, 2,4-F_2Ph C-1), 128.68 (C-3′ and C-5′), 130.44 (m, 2,4-F_2Ph C-6), 131.17 (C-2′ and C-6′), 132.11 (C-4′), 137.12 (C-1′), 145.45 (C-5 triazole), 151.11 (C-3 triazole), 159.41 (dd, $J_{C,F}$ = 246.6

and 12.3 Hz, 2,4-F_2Ph C-2), 162.39 (dd, $J_{C,F}$ = 245.1 and 12.6 Hz, 2,4-F_2Ph C-4), 195.07 (C═S). MS (*m/z*, %): 523 (M^+, < 1), 334 (8), 209 (31), 182 (8), 168 (9), 154 (18), 139 (16), 125 (100), 99 (6), 83 (34), 56 (14). Anal. Calcd for $C_{23}H_{24}ClF_2N_5OS_2$: C, 52.72; H, 4.62; N, 13.36. Found: 52.91; H, 4.49; N, 13.55.

*4.2.3. 2-(2,4-Difluorophenyl)-2-hydroxy-3-(1H-1,2,4-triazol-1-yl)propyl 4-(2,4-dichlorobenzyl)piperazine-1-carbodithioate (**6c**)*

Yield: 62%; mp: 113–115 °C; IR (ν_{max}, cm^{-1}): 3208, 3069, 2713, 1615, 1502, 1416, 1308, 1224; 1114, 1087, 1030, 966, 676, 514, 479. ^{1}H NMR (400 MHz, $CDCl_3$) δ: 2.54–2.63 (m, 4H, piperazine), 3.62 (s, 2H, CH_2 benzylic), 3.86–3.99 (m, 2H, piperazine), 4.01 (d, 1H, J = 14.8 Hz, H_a), 4.29 (d, 1H, J = 14.8 Hz, H_b), 4.31–4.41 (m, 2H, piperazine), 4.68 (d, 1H, J = 14.4 Hz, H_c), 4.72 (d, 1H, J = 14.4 Hz, H_d), 5.32 (s, 1H, OH), 6.80–6.88 (m, 2H, H-3 and H-5), 7.25 (dd, 1H, J = 8.2 and 2.0 Hz, H-5′), 7.39 (d, 1H, J = 8.4 Hz, H-6′), 7.40 (d, 1H, J = 2.0 Hz, H-3′), 7.56–7.62 (m, 1H, H-6), 7.85 (s, 1H, triazole), 8.13 (s, 1H, triazole). ^{13}C NMR (100 MHz, DMSO-d_6) δ: 46.60 (CH_2-S), 50.14 (1C, piperazine), 52.41 (2C, piperazine), 53.08 (1C, piperazine), 56.76 (C-OH), 57.76 (CH_2 benzylic), 73.70 (CH_2-N), 104.56 (t, $J_{C,F}$ = 27.5 Hz, 2,4-F_2Ph C-3), 111.35 (d, $J_{C,F}$ = 23.2 Hz, 2,4-F_2Ph C-5), 125.41 (dd, $J_{C,F}$ = 13.0 and 3.8 Hz, 2,4-F_2Ph C-1), 127.71 (C-5′), 129.22 (C-3′), 130.45 (m, 2,4-F_2Ph C-6), 132.70 (C-6′), 132.88 (C-4′), 134.72 (C-1′), 134.79 (C-2′), 145.46 (C-5 triazole), 151.11 (C-3 triazole), 159.41 (dd, $J_{C,F}$ = 246.3 and 12.3 Hz, 2,4-F_2Ph C-2), 162.40 (dd, $J_{C,F}$ = 244.6 and 12.7 Hz, 2,4-F_2Ph C-4), 195.13 (C═S). MS (*m/z*, %): 557 (M^+, < 1), 404 (3), 243 (33), 221 (24), 202 (16), 188 (19), 173 (8), 159 (100), 141 (16), 127 (28), 101 (12), 86 (40), 70 (6), 56 (12). Anal. Calcd for $C_{23}H_{23}Cl_2F_2N_5OS_2$: C, 49.46; H, 4.15; N, 12.54. Found: C, 49.64; H, 4.11; N, 12.70.

*4.2.4. 2-(2,4-Difluorophenyl)-2-hydroxy-3-(1H-1,2,4-triazol-1-yl)propyl 4-(3,4- dichlorobenzyl)piperazine-1-carbodithioate (**6d**)*

Yield: 61%; mp: 127–130 °C; IR (ν_{max}, cm^{-1}): 3233, 2824, 1615, 1514, 1499, 1471, 1273, 1225, 1137, 1030, 964, 965, 818, 676, 535, 511, 459. ^{1}H NMR (400 MHz, $CDCl_3$) δ: 2.46–2.60 (m, 4H, piperazine), 3.49 (s, 2H, CH_2 benzylic), 3.84–3.98 (m, 2H, piperazine), 4.00 (d, 1H, J = 15.2 Hz, H_a), 4.28 (d, 1H, J = 15.2 Hz, H_b), 4.31–4.42 (m, 2H, piperazine), 4.67 (d, 1H, J = 14.0 Hz, H_c), 4.72 (d, 1H, J = 14.4 Hz, H_d), 5.32 (s, 1H, OH), 6.79–6.88 (m, 2H, H-3 and H-5), 7.16 (dd, 1H, J = 8.2 and 1.6 Hz, H-6′), 7.41 (d, 1H, J = 8.0 Hz, H-5′), 7.44 (d, 1H, J = 1.6 Hz, H-2′), 7.55–7.62 (m, 1H, H-6), 7.84 (s, 1H, triazole), 8.13 (s, 1H, triazole). ^{13}C NMR (100 MHz, DMSO-d_6): 45.94 (2C, piperazine and 1C, CH_2-S), 46.96 (CH_2 benzylic), 51.15 (1C, piperazine), 52.40 (1C, piperazine), 56.75 (C-OH), 73.66 (CH_2-N), 104.57 (t, $J_{C,F}$ = 27.0 Hz, 2,4-F_2Ph C-3), 111.39 (d, $J_{C,F}$ = 18.4 Hz, 2,4-F_2Ph C-5), 125.37 (d, $J_{C,F}$ = 12.8 Hz, 2,4-F_2Ph C-1), 130.41 (C-6′), 130.46 (C-5′), 130.56 (C-2′), 131.17 (m, 2,4-F_2Ph C-6), 131.21 (C-4′), 131.61 (C-3′), 131.64 (C-1′), 145.54 (C-5 triazole), 151.12 (C-3 triazole), 159.41 (dd, $J_{C,F}$ = 245.7 and 12.3 Hz, 2,4-F_2Ph C-2), 162.41 (dd, $J_{C,F}$ = 245.1 and 12.6 Hz, 2,4-F_2Ph C-4), 196.19 (C═S). MS (*m/z*, %): 557 (M^+, < 1), 221 (11), 202 (7), 187 (7), 159 (11), 141 (15), 127 (24), 101 (23), 86 (100), 72 (7), 58 (22). Anal. Calcd for $C_{23}H_{23}Cl_2F_2N_5OS_2$: C, 49.46; H, 4.15; N, 12.54. Found: C, 49.65; H, 4.22; N, 12.57.

*4.2.5. 2-(2,4-Difluorophenyl)-2-hydroxy-3-(1H-1,2,4-triazol-1-yl)propyl 4-(2,6- dichlorobenzyl)piperazine-1-carbodithioate (**6e**)*

Yield: 69%; mp: 110–113 °C; IR (ν_{max}, cm^{-1}): 3696, 3662, 3239, 2920, 2810, 1616, 1597, 1498, 1435, 1272, 1227, 1136, 1102, 992, 964, 763, 673, 511. ^{1}H NMR (400 MHz, $CDCl_3$) δ: 2.61–2.71 (m, 4H, piperazine), 3.81 (s, 2H, CH_2 benzylic), 3.86–3.92 (m, 2H, piperazine), 4.01 (d, 1H, J = 14.8 Hz, H_a), 4.22–4.38 (m, 2H, piperazine), 4.29 (d, 1H, J = 15.2 Hz, H_b), 4.68 (d, 1H, J = 14.0 Hz, H_c), 4.72 (d, 1H, J = 14.0 Hz, H_d), 5.35 (br s, 1H, OH), 6.80–6.88 (m, 2H, H-3 and H-5), 7.19 (t, 1H, J = 8.0 Hz, H-4′), 7.33 (d, 2H, J = 8.0 Hz, H-3′ and H-5′), 7.56–7.62 (m, 1H, H-6), 7.84 (s, 1H, triazole), 8.14 (s, 1H, triazole). ^{13}C NMR (100 MHz, DMSO-d_6) δ: 46.62 (CH_2-S), 50.30 (1C, piperazine), 51.54 (1C, piperazine), 52.49 (2C, piperazine), 55.83 (C-OH), 56.80 (CH_2 benzylic), 73.76 (CH_2-N), 104.55 (dd, $J_{C,F}$ = 26.7 and 25.7 Hz, 2,4-F_2Ph C-3), 111.34 (d, $J_{C,F}$ = 19.2 Hz, 2,4-F_2Ph C-5), 125.41 (dd, $J_{C,F}$ = 9.2 and 2.8 Hz, 2,4-F_2Ph C-1), 129.14 (C-3′ and C-5′), 130.47 (m, 2,4-F_2Ph C-6), 130.58 (C-4′), 133.56 (C-1′), 136.60 (C-2′ and C-6′), 145.46 (C-5 triazole), 151.11 (C-3 triazole), 159.42 (dd, $J_{C,F}$ = 246.2 and 12.2 Hz, 2,4-F_2Ph C-2), 162.40 (dd, $J_{C,F}$ = 245.00 and 12.4 Hz, 2,4-F_2Ph C-4), 194.95 (C═S). MS (*m/z*, %): 557 (M^+, < 1), 404 (6), 243 (39), 221 (16), 202 (46), 188 (16), 159 (100), 139 (13), 123 (13), 89 (12), 71 (5), 56 (22). Anal. Calcd for $C_{23}H_{23}Cl_2F_2N_5OS_2$: C, 49.46; H, 4.15; N, 12.54. Found: C, 49.32; H, 3.99; N, 12.38.

*4.2.6. 2-(2,4-Difluorophenyl)-2-hydroxy-3-(1H-1,2,4-triazol-1-yl)propyl 4-(4-bromobenzyl)piperazine-1-carbodithioate (**6f**)*

Yield: 63%; mp: 138–140 °C; IR (ν_{max}, cm^{-1}): 3696, 3239, 2920, 2910, 1597, 1616, 1498, 1435, 1272, 1227, 1136, 1102, 922, 964, 848, 703, 676. ^{1}H NMR (400 MHz, $CDCl_3$) δ: 2.45–2.61 (m, 4H, piperazine), 3.49 (s, 2H, CH_2 benzylic), 3.85–3.98 (br s, 2H, piperazine), 4.01 (d, 1H, J = 15.2 Hz, H_a), 4.29 (d, 1H, J = 15.2 Hz, H_b), 4.31–4.43 (m, 2H, piperazine), 4.67 (d, 1H, J = 14.0 Hz, H_c), 4.72 (d, 1H, J = 14.0 Hz, H_d), 5.33 (s, 1H, OH), 6.82–6.88 (m, 2H, H-3 and H-5), 7.20 (d, 2H, J = 8.4 Hz, H-2′ and H-6′), 7.47 (d, 2H, J = 8.4 Hz, H-3′ and H-5′), 7.56–7.62 (m, 1H, H-6), 7.85 (s, 1H, triazole), 8.14 (s, 1H, triazole). ^{13}C NMR (100 MHz, $CDCl_3$) δ: 43.67 (d, $J_{C,F}$ = 4.0 Hz, CH_2-S), 50.48 (1C, piperazine), 52.23 (2C, piperazine), 52.48 (1C, piperazine), 57.06 (d, $J_{C,F}$ = 4.9 Hz, C-OH), 61.62 (CH_2 benzylic), 75.39 (d, $J_{C,F}$ = 5.0 Hz, CH_2-N), 104.24 (t, $J_{C,F}$ = 26.9 Hz, 2,4-F_2Ph C-3), 111.59 (dd, $J_{C,F}$ = 20.5 and 3.2 Hz, 2,4-F_2Ph C-5), 121.33 (C-4′), 124.66 (dd, $J_{C,F}$ = 13.9 and 3.5 Hz, 2,4-F_2Ph C-1), 130.37 (dd, $J_{C,F}$ = 9.5 and 5.5 Hz, 2,4-F_2Ph C-6), 130.66 (C-2′ and C-6′), 131.57 (C-3′ and C-5′), 136.29 (C-1′), 144.58 (C-5 triazole), 151.45 (C-3 triazole), 158.71 (dd, $J_{C,F}$ = 245.2 and 12.0 Hz, 2,4-F_2Ph C-2), 162.89 (dd, $J_{C,F}$ = 248.9 and 12.4 Hz, 2,4-F_2Ph C-4), 197.65 (C═S). MS (*m/z*, %): 567 (M^+, < 1), 424 (10), 314 (3), 253 (45). 234 (12), 221 (47), 197 (23), 182 (61), 169 (100), 171 (98), 154 (20), 139 (40), 119 (30), 102 (9), 90 (45), 78 (81), 56 (94). Anal. Calcd for $C_{23}H_{24}BrF_2N_5OS_2$: C, 48.59; H, 4.26; N, 12.32. Found: C, 48.60; H, 4.37; N, 12.30.

*4.2.7. 2-(2,4-Dichlorophenyl)-2-hydroxy-3-(1H-1,2,4-triazol-1-yl)propyl 4-(3- chlorobenzyl)piperazine-1-carbodithioate (**6g**)*

Yield: 53%; mp: 120–124 °C; IR (ν_{max}, cm^{-1}): 2925, 1515, 1469, 1421, 128, 1225, 1133, 1019, 598, 810. ^{1}H NMR (400 MHz, DMSO-d_6) δ: 2.80–3.42 (m, 4H, piperazine), 3.60–4.02 (m, 3H, piperazine), 4.05 (d, 1H, J = 13.2 Hz, H_a), 4.32 (s, 2H, CH_2 benzylic), 4.38 (m, 1H, piperazine), 4.40 (d, 1H, J = 13.2 Hz, H_b), 4.88 (d, 1H, J = 14.4 Hz, H_c), 5.10 (d, 1H, J = 14.4 Hz, H_d), 7.33 (dd, 1H, J = 8.8 and 2.0 Hz, H-5), 7.36–7.40 (m, 1H, H-6′), 7.47 (d, 1H, J = 8.8 Hz, H-6), 7.53 (t, 1H, J = 8.8 Hz, H-5′), 7.58 (d, 1H, J = 2.4 Hz, H-3), 7.61–7.76 (2H, m, H-2′, and H-4′), 8.05 (s, 1H, triazole), 8.34 (s, 1H, triazole). ^{13}C NMR (100 MHz, DMSO-d_6) δ: 46.08 (CH_2-S), 47.50 (1C, piperazine), 50.04 (2C, piperazine), 50.48 (1C, piperazine), 55.64 (C-OH), 57.80 (CH_2 benzylic), 74.65 (CH_2-N), 127.53 (C-5′), 128.85 (C-5), 129.25 (C-6′), 130.35 (C-4′), 131.41 (C-6), 131.69 (C-3), 133.73 (C-2′), 133.85 (C-2), 133.97 (C-4), 134.90 (C-3′), 137.69 (C-1′), 145.06 (C-1), 149.09 (C-5 triazole), 151.84 (C-3 triazole), 196.92 (C═S). MS (*m/z*, %): 555 (M^+, < 1), 407 (3), 314 (5), 270 (50), 252 (41), 235 (43), 219 (21), 203 (14), 187 (12), 160 (14), 128 (18), 98 (5), 83 (100), 64 (29). Anal. Calcd for $C_{23}H_{24}Cl_3N_5OS_2$: C, 49.60; H, 4.34; N, 12.57. Found: C, 49.49; H, 4.35; N, 12.50.

*4.2.8. 2-(2,4-Dichlorophenyl)-2-hydroxy-3-(1H-1,2,4-triazol-1-yl)propyl 4-(2,4- dichlorobenzyl)piperazine-1-carbodithioate (**6h**)*

Yield: 58%; mp: 100–104 °C; IR (ν_{max}, cm^{-1}): 3221, 2922, 1704, 1527, 1505, 1471, 1421, 1274, 1228, 1139, 1049, 995, 969, 806, 677, 454. ^{1}H NMR (400 MHz, $CDCl_3$) δ: 2.49–2.65 (m, 4H, piperazine), 3.47

(br s, 1H, piperazine), 3.62 (s, 1H, CH_2 benzylic), 3.82–3.99 (m, 2H, piperazine), 4.29 (d, 1H, J = 14.8 Hz, H_a), 4.40 (br s, 1H, piperazine), 4.43 (d, 1H, J = 14.8 Hz, H_b), 4.88 (d, 1H, J = 14.0 Hz, H_c), 4.95 (d, 1H, J = 14.0 Hz, H_d), 5.48 (s, 1H, OH), 7.26 (d, 1H, J = 2.0 Hz, H-3), 7.23 (dd, 1H, J = 6.8 and 2.0 Hz, H-5′), 7.25 (dd, 1H, J = 6.4 and 2.0 Hz, H-5), 7.38 (d, 1H, J = 8.0 Hz, H-6′), 7.39–7.41 (m, 2H, H-3 and H-3′), 7.75 (d, 1H, J = 8.8 Hz, H-6), 7.85 (s, 1H, triazole), 8.16 (s, 1H, triazole). ^{13}C NMR (100 MHz, DMSO-d_6): 45.56 (CH_2-S), 51.40 (1C, piperazine), 52.19 (1C, piperazine), 52.42 (2C, piperazine), 55.46 (C-OH), 57.77 (CH_2 benzylic), 74.92 (CH_2-N), 127.42 (C-5′), 127.71 (C-5), 129.22 (C-6), 130.48 (C-3′), 131.40 (C-3), 131.73 (C-6′), 132.70 (C-2), 132.88 (C-4), 133.57 (C-4′), 134.73 (C-1′), 134.80 (C-2′), 138.06 (C-1), 145.53 (C-5 triazole), 151.11 (C-3 triazole), 195.08 (C═S). MS (*m/z*, %): 589 (M^+, < 1), 279 (7), 256 (40), 218 (73), 202 (48), 181 (23), 159 (100), 145 (5), 128 (25), 113 (9), 99 (13), 85 (15), 64 (42). Anal. Calcd for $C_{23}H_{23}Cl_4N_5OS_2$: C, 46.71; H, 3.92; N, 11.84. Found: C, 46.92; H, 3.85; N, 11.61.

4.2.9. 2-(2,4-Dichlorophenyl)-2-hydroxy-3-(1H-1,2,4-triazol-1-yl)propyl 4-(3,4- dichlorobenzyl)piperazine-1-carbodithioate (6i)

Yield: 54%; mp: 132–135 °C; IR (ν_{max}, cm^{-1}): 3380, 2543, 1708, 1556, 1467, 1416, 1373, 1252, 1210, 1090, 1016, 954, 808, 502, 484. ^{1}H NMR (400 MHz, $CDCl_3$) δ: 2.40–2.60 (m, 4H, piperazine), 3.49 (s, 2H, CH_2 benzylic), 3.83–4.01 (m, 2H, piperazine), 4.23–4.30 (m, 1H, piperazine), 4.28 (d, 1H, J = 15.2 Hz, H_a), 4.32–4.42 (m, 1H, piperazine), 4.43 (d, 1H, J = 15.2 Hz, H_b), 4.88 (d, 1H, J = 14.4 Hz, H_c), 4.95 (d, 1H, J = 14.4 Hz, H_d), 5.48 (s, 1H, OH), 7.16 (dd, 1H, J = 8.0 and 2.0 Hz, H-5′), 7.23 (dd, 1H, J = 8.8 and 2.0 Hz, H-5), 7.38–7.46 (m, 3H, H-3, H-2′ and H-6′), 7.75 (d, 1H, J = 8.4 Hz, H-6), 7.86 (s, 1H, triazole), 8.16 (s, 1H, triazole). ^{13}C NMR (100 MHz, DMSO-d_6) δ: 45.54 (CH_2-S), 51.44 (1C, piperazine), 52.27 (2C, piperazine), 52.88 (1C, piperazine), 55.44 (C-OH), 60.11 (CH_2 benzylic), 74.89 (CH_2-N), 127.42 (C-5), 129.60 (C-6), 130.07 (C-3′),130.47 (C-6′), 130.82 (C-5′), 130.88 (C-2′), 131.10 (C-3), 131.37 (C-4′), 131.72 (C-2), 133.57 (C-4), 138.05 (C-1′), 139.54 (C-1), 145.54 (C-5 triazole), 151.11 (C-3 triazole), 195.03 (C═S). MS (*m/z*, %): 589 (M^+, < 1), 252 (27), 218 (41), 202 (62), 181 (75), 159 (100), 123 (14), 101 (4), 85 (14), 56 (20). Anal. Calcd for $C_{23}H_{23}Cl_4N_5OS_2$: C, 46.71; H, 3.92; N, 11.84. Found: C, 46.69; H, 4.12; N, 11.88.

4.3. Antifungal susceptibility testing against different Candida species

The minimum inhibitory concentration (MIC) values of test compounds **6a-i** and fluconazole (Pfizer, Groton, CT, USA) were determined by micro-dilution method as recommended by Clinical and Laboratory Standards Institute (CLSI) M27-A3 and M27-S4 documents [19,20]. The detailed procedure for MICs determination was included in the Supplementary Material.

4.4. Hemolysis assay

The hemolytic activity of selected compound **6b** and fluconazole was evaluated using method described by Carter et al. [24]. Fresh whole human blood was collected into dipotassium EDTA-coated Vacutainer tubes and centrifuged at 500 g for 5 min. The red blood cell pellets were washed in saline solution (two times) and then in phosphate-buffered saline (PBS). The washed erythrocytes were re-diluted in PBS (1:25). On the other hand, different concentrations of compounds were prepared in DMSO and an aliquot (10 μL) of each concentration was added to diluted erythrocytes (190 μL) in a 96-well plate, giving final concentrations of 1, 10 and 50 μg/mL in triplicate. DMSO and Triton X-100 (2% v/v) were included as negative and positive controls, respectively. The plate was incubated at 37 °C for 1 h and then cell suspensions were centrifuged at 500 g. After collecting each supernatant (100 μL), their absorbance were measured at 451 nm. The percentage of hemolysis was determined as follow:

$$\%\text{Hemolysis} = [(A_{\text{sample}} - A_{\text{blank}})/(A_{\text{positive control}})] \times 100$$

4.5. Viability assay of HepG2 cells

HepG2 (Human hepatocarcinoma) cell line was purchased from Pasture Institute of Iran. Viability of HepG2 cells was determined by MTT assay after exposure to test compound **6b** and fluconazole (at concentrations of 25, 50, 100, and 200 μg/mL). DMSO and cisplatin were used as negative and positive controls, respectively. The detailed procedure for MTT assay was included in the Supplementary Material.

4.6. Computational study

The X-ray crystal structures of CYP51 in complex with itraconazole (PDB ID: 5JLC for *C. glabrata* and 5V5Z for *C. albicans*) were obtained from the RCSB Protein Data Bank. AutoDockTools (ADT) 1.5.4 package was used for preparing all input files. Any crystallographic water, if present was eliminated and hydrogens were added to the structure. The 3D structure of the compound was constructed and subjected to energy minimization by MOPAC Chem3D Ultra 8.0.3. Assigning appropriate charge and the heme cofactor and the iron charges were carefully inspected. To define the active site for docking, the receptor-grid was generated with grid box size of 60 × 60 × 60 with the spacing value of 0.375. The detailed docking methodology has been described previously [15].

Acknowledgement

This work was supported by a grant from the Research Council of Mazandaran University of Medical Sciences, Sari, Iran (Grant No. 552). This work was related to the Pharm.D. thesis of YM (Faculty of Pharmacy, Mazandaran University of Medical Sciences).

Appendix A. Supplementary material

Supplementary data to this article can be found online at https://doi.org/10.1016/j.bioorg.2019.103060.

References

[1] National Institutes of Health (US), Biological Sciences Curriculum Study, NIH Curriculum Supplement Series [Internet], Bethesda (MD): National Institutes of Health (US), 2007. Understanding Emerging and Re-emerging Infectious Diseases. Available from: https://www.ncbi.nlm.nih.gov/books/NBK20370/.
[2] L.K. Dropulic, H.M. Lederman, Overview of infections in the immunocompromised host, Microbiol. Spectr. 4 (2016), https://doi.org/10.1128/microbiolspec.DMIH2-0026-2016.
[3] J. Tanwar, S. Das, Z. Fatima, S. Hameed, Multidrug resistance: an emerging crisis, Interdiscip. Perspect. Infect. Dis. 2014 (2014) 541340, , https://doi.org/10.1155/2014/541340.
[4] C.J. Seneviratne, E.A.R. Rosa, Editorial: antifungal drug discovery: new theories and new therapies, Front. Microbiol. 7 (2016) 728, https://doi.org/10.3389/fmicb.2016.00728.
[5] M.K. Kathiravan, A.B. Salake, A.S. Chothe, P.B. Dudhe, R.P. Watode, M.S. Mukta, S. Gadhwe, The biology and chemistry of antifungal agents: a review, Bioorg. Med. Chem. 20 (2012) 5678–5698, https://doi.org/10.1016/j.bmc.2012.04.045.
[6] S. Emami, P. Tavangar, M. Keighobadi, An overview of azoles targeting sterol 14α-demethylase for antileishmanial therapy, Eur. J. Med. Chem. 135 (2017) 241–259, https://doi.org/10.1016/j.ejmech.2017.04.044.
[7] G.I. Lepesheva, M.R. Waterman, Sterol 14α-demethylase cytochrome P450 (CYP51), a P450 in all biological kingdoms, Biochim. Biophys. Acta 1770 (2007) 467–477, https://doi.org/10.1016/j.bbagen.2006.07.018.
[8] L.R. Peyton, S. Gallagher, M. Hashemzadeh, Triazole antifungals: a review, Drugs Today 51 (2015) 705–718, https://doi.org/10.1358/dot.2015.51.12.2421058.
[9] R.E. Lewis, Current concepts in antifungal pharmacology, Mayo Clin. Proc. 86 (2011) 805–817, https://doi.org/10.4065/mcp.2011.0247.
[10] S.M. Hashemi, H. Badali, H. Irannejad, M. Shokrzadeh, S. Emami, Synthesis and biological evaluation of fluconazole analogs with triazole-modified scaffold as potent antifungal agents, Bioorg. Med. Chem. 23 (2015) 1481–1491, https://doi.org/10.1016/j.bmc.2015.02.011.
[11] V. Bala, G. Gupta, V.L. Sharma, Chemical and medicinal versatility of dithiocarbamates: an overview, Mini Rev. Med. Chem. 14 (2014) 1021–1032.
[12] L. Kumar, N. Lal, V. Kumar, A. Sarswat, S. Jangir, V. Bala, L. Kumar, B. Kushwaha,

A.K. Pandey, M.I. Siddiqi, P.K. Shukla, J.P. Maikhuri, G. Gupta, V.L. Sharma, Azole-carbodithioate hybrids as vaginal anti-*Candida* contraceptive agents: design, synthesis and docking studies, Eur. J. Med. Chem. 70 (2013) 68–77.

[13] S.M. Monti, A. Maresca, F. Viparelli, F. Carta, G. De Simone, F.A. Mühlschlegel, A. Scozzafava, C.T. Supuran, Dithiocarbamates are strong inhibitors of the beta-class fungal carbonic anhydrases from *Cryptococcus neoformans*, *Candida albicans* and *Candida glabrata*, Bioorg. Med. Chem. Lett. 22 (2012) 859–862.

[14] S.M. Hashemi, H. Badali, M.A. Faramarzi, N. Samadi, M.H. Afsarian, H. Irannejad, S. Emami, Novel triazole alcohol antifungals derived from fluconazole: design, synthesis, and biological activity, Mol. Divers. 19 (2015) 15–27, https://doi.org/10.1007/s11030-014-9548-0.

[15] K. Motahari, H. Badali, S.M. Hashemi, H. Fakhim, H. Mirzaei, A. Vaezi, M. Shokrzadeh, S. Emami, Discovery of benzylthio analogs of fluconazole as potent antifungal agents, Future Med. Chem. 10 (2018) 987–1002, https://doi.org/10.4155/fmc-2017-0295.

[16] H. Fakhim, S. Emami, A. Vaezi, S.M. Hashemi, L. Faeli, K. Diba, E. Dannaoui, H. Badali, In vitro activities of novel azole compounds ATTAF-1 and ATTAF-2 against fluconazole-susceptible and -resistant isolates of Candida species, pii: e01106-16, Antimicrob. Agents Chemother. 61 (2016), https://doi.org/10.1128/AAC.01106-16.

[17] M.H. Miceli, J.A. Diaz, S.A. Lee, Emerging opportunistic yeast infections, Lancet Infect. Dis. 11 (2011) 142–151.

[18] M. Xiao, X. Fan, S.C.A. Chen, H. Wang, Z.Y. Sun, K. Liao, S.L. Chen, Y. Yan, M. Kang, Z.D. Hu, Y.Z. Chu, T.S. Hu, Y.X. Ni, G.L. Zou, F. Kong, Y.C. Xu, Antifungal susceptibilities of Candida glabrata species complex, Candida krusei, Candida parapsilosis species complex and Candida tropicalis causing invasive candidiasis in China: 3 year national surveillance, J. Antimicrob. Chemother. 70 (2015) 802–810.

[19] Clinical and Laboratory Standards Institute, Reference method for broth dilution antifungal susceptibility testing of yeasts, approved standard 3rd ed., Document M27-A3, Clinical and Laboratory Standards Institute, Wayne, PA, 2008.

[20] Clinical and Laboratory Standards Institute, Reference method for broth dilution antifungal susceptibility testing of yeasts, 4th informational supplement, Document M27-S4, Clinical and Laboratory Standards Institute, Wayne, PA, 2012.

[21] I. Kyriakidis, A. Tragiannidis, S. Munchen, A.H. Groll, Clinical hepatotoxicity associated with antifungal agents, Expert Opin. Drug Saf. 16 (2017) 149–165.

[22] F.P. Tverdek, D. Kofteridis, D.P. Kontoyiannis, Antifungal agents and liver toxicity: a complex interaction, Expert Rev. Anti Infect. Ther. 14 (2016) 765–776.

[23] H.B. Borate, S.R. Maujan, S.P. Sawargave, M.A. Chandavarkar, S.R. Vaiude, V.A. Joshi, R.D. Wakharkar, R. Iyer, R.G. Kelkar, S.P. Chavan, S.S. Kunte, Fluconazole analogues containing 2H–1,4-benzothiazin-3(4H)-one or 2H–1,4-benzoxazin-3(4H)-one moieties, a novel class of anti-*Candida* agents, Bioorg. Med. Chem. Lett. 20 (2010) 722–725, https://doi.org/10.1016/j.bmcl.2009.11.071.

[24] G.P. Carter, J.R. Harjani, L. Li, N.P. Pitcher, Y. Nong, T.V. Riley, D.A. Williamson, T.P. Stinear, J.B. Baell, B.P. Howden, 1,2,4-Oxadiazole antimicrobials act synergistically with daptomycin and display rapid kill kinetics against MDR Enterococcus faecium, Antimicrob. Chemother. 73 (2018) 1562–1569.